Highly sensitive amperometric biosensor based on electrochemically-reduced graphene oxide-chitosan/hemoglobin nanocomposite for nitromethane determination

Yunping Wen, Wei Wen, Xiuhua Zhang, Shengfu Wang

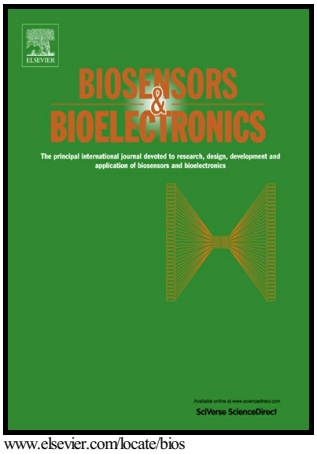

www.elsevier.com/locate/bios

PII: S0956-5663(16)30026-4
DOI: http://dx.doi.org/10.1016/j.bios.2016.01.028
Reference: BIOS8368

To appear in: *Biosensors and Bioelectronic*

Received date: 19 October 2015
Revised date: 17 December 2015
Accepted date: 10 January 2016

Cite this article as: Yunping Wen, Wei Wen, Xiuhua Zhang and Shengfu Wang, Highly sensitive amperometric biosensor based on electrochemically-reduce graphene oxide-chitosan/hemoglobin nanocomposite for nitromethan determination, *Biosensors and Bioelectronic* http://dx.doi.org/10.1016/j.bios.2016.01.028

Highly Sensitive Amperometric Biosensor Based on Electrochemically-reduced Graphene Oxide-Chitosan/ Hemoglobin Nanocomposite for Nitromethane Determination

Yunping Wen, Wei Wen*, Xiuhua Zhang, Shengfu Wang*

Hubei Collaborative Innovation Center for Advanced Organic Chemical Materials, Ministry of Education Key Laboratory for the Synthesis and Application of Organic Functional Molecules & College of Chemistry and Chemical Engineering, Hubei University, Wuhan 430062, PR China

*Corresponding author.

Telephone: +86-27-50865309; Fax: +86-27-88663043; E-mail address: wenwei@hubu.edu.cn; wangsf@hubu.edu.cn.

Abstract

Nitromethane (CH_3NO_2) is an important organic chemical raw material with a wide variety of applications as well as one of the most common pollutants. Therefore it is pretty important to establish a simple and sensitive detection method for CH_3NO_2. In our study, a novel amperometric biosensor for nitromethane (CH_3NO_2) based on immobilization of electrochemically-reduced graphene oxide (rGO), chitosan (CS) and hemoglobin (Hb) on a glassy carbon electrode (GCE) was constructed. Scanning electron microscopy, infrared spectroscopy and electrochemical methods were used to characterize the Hb-CS/rGO-CS composite film. The effects of scan rate

and pH of phosphate buffer on the biosensor have been studied in detail and optimized. Due to the graphene and chitosan nanocomposite, the developed biosensor demonstrating direct electrochemistry with faster electron-transfer rate (6.48 s^{-1}) and excellent catalytic activity towards CH_3NO_2. Under optimal conditions, the proposed biosensor exhibited fast amperometric response (< 5 s) to CH_3NO_2 with a wide linear range of 5 μM ~ 1.46 mM (R = 0.999) and a low detection limit of 1.5 μM (S/N=3). In addition, the biosensor had high selectivity, reproducibility and stability, providing the possibility for monitoring CH_3NO_2 in complex real samples.

Keywords: Electrochemically-reduced graphene oxide; Graphene-chitosan/hemoglobin nanocomposite; Direct electrochemistry; Nitromethane; Electrochemical biosensor.

1. Introduction

Organic nitro compounds are important material of organic chemistry industry, which are widely used in the production of pharmacy, fuel, explosives, fiber, pesticides and fine chemicals. Nitromethane (CH_3NO_2) is the simplest organic nitro compounds and a popular energy material with versatile applications. It is also a common chemical pollutant, which is flammable, explosive and toxic. Nitromethane is mainly harmful to central nervous system, damage liver and kidney, and may also cause methemoglobinemia. In addition, over-inhalhation of CH_3NO_2 can lead to acute poisoning such as dizziness, limb weakness, dyspnea and unconsciousness (Page et al.,

2001). Therefore, diverse strategies have been employed to the study of nitromethane including solid-phase microextraction (SPME)-gas chromatography (GC)-high resolution mass spectrometry (HRMS) (SPME-GC-HRMS)(Alwis et al., 2008), colorimetry (Jones and Riddick, 1951) and fluorimetry (Meaney and McGuffin, 2008). However, most of these methods are more or less flawed. For example, fluorescence spectrometry of high sensitivity requires plenty samples. Meanwhile there are few reports about the determination of CH_3NO_2 by the electrochemical method, which is fast, inexpensive and of high sensitivity and selectivity.

As a special kind of sensor, biosensor developed in 1960s is a new analysis and measurement technology and has become a broad and dynamic research field. Among a wide variety of biosensors, electrochemical enzyme biosensor is always the mainstream of research, which manages to combine the fast and sensitivity electrochemical method with the intrinsic chemical specificity and signal amplification function of the enzyme judiciously together. It is to be observed that hemoglobin (Hb) is often used as a model molecule for studying the electrochemistry and electrocatalysis of proteins. Hemoglobin, an important redox heme protein in red blood cells, is one of the most studied proteins in structure. It consists of four chains including two α chains and two β chains, and on every chain there are heme molecules containing iron atoms, which can combine with O_2 and then transport it in the blood. Owing to easy availability, clear structure and low cost, hemoglobin is widely studied as the ideal model of researching direct electrochemistry of biosensor to proteins. However, direct electron transfer between Hb and the traditional bare electrodes is extremely difficult to achieve for several reasons (Léger and Bertrand, 2008). Firstly, the structure of hemoglobin is complex and electroactive centers buried in polypeptides are far away from the electrode. Secondly, the instability of Hb makes it easy to

cause the protein denaturation on the electrode surface. Thirdly, the adsorption of Hb molecules with large three-dimensional structure would lead to electrode passivation. In order to achieve the direct electron transfer of Hb, seeking satisfactory electrode materials and new enzyme immobilization methods become the breakthrough. Film entrapment is the most attractive method in recent years, which modifies proteins together with the materials such as nanomaterials (Xu et al., 2009), biopolymers (Liu et al., 2004), surfactant (Lu et al., 2007) on the electrode, providing proteins with an appropriate and stable microenvironment to maintain their activity and enhancing the electron transfer between proteins and electrodes.

Graphene, as a new carbon nanomaterial, has become a hot spot in various research areas due to the special physicochemical properties since its discovery (Geim and Novoselov, 2007; Allen et al., 2010; Sabourin et al., 2009). Graphene is one-atom-thick and two-dimensional sheets composed of carbon atoms in the sp^2 hybrid orbitals. It has high specific surface area, excellent electrical conductivity and good biocompatibility (Novoselov et al., 2004). With the aforementioned advantages, graphene has received considerable attention as a support material in the fabrication of electrochemical sensors (Alwarappan et al., 2009; Shan et al., 2009; Stankovich et al., 2006). However, graphene sheets have a tendency to stack into graphite by the attraction of Van der Waals force (Li et al., 2008). Additionally, the native hydrophobicity makes graphene difficult to disperse in aqueous media. So far, graphene can be prepared by chemical, thermal or electrochemical methods (Gao et al., 2010; Guo et al., 2009). Chemical exfoliation method much prefers the mass production but involves the use of toxic reductant and the produced graphene sheets are not suitable for nanoelectronic applications (Park and Ruoff, 2009), whereas thermal method demands high temperatures. Therefore, electrochemical method that serves as an

alternative approach is more green and efficient (Dong et al., 2012; Lin et al., 2012). Graphene oxide (GO), the oxygenated derivative of graphite, is a versatile dispersant because it is an amphiphilic molecule with hydrophilicity and hydrophobicity, but GO have the native insulating poverty because of its aliphatic sp^3 hybridized domain. However, the reductive product (electrochemically reduced graphene oxide, rGO) with good conductivity is a unique and promising material in diverse applications. Therefore, GO with good solubility was reduced by the electrochemical method to be the conductive rGO. Chitosan (CS), a natural polysaccharide polymer, has attracted great attention due to its excellent biological compatibility, good hydrophilicity and film-forming ability (Lu et al., 2006; Peniche et al., 2003), which can provide proteins with a suitable and biocompatible microenvironment. But in consideration of its relatively poor conductivity, chitosan is often associated with conductive materials such as carbon materials, ionic liquid, redox mediators and metal nanomaterials to form composite film for immobilizing proteins (Kang et al., 2009; Zhang et al., 2004). In this paper, graphene with excellent conductivity and chitosan with good biological compatibility are combined to entrap Hb and construct a novel hemoglobin electrochemical biosensor.

In this work, graphene was creatively produced by the electrochemical reduction method, and rGO-CS matrix was served as a preeminent immobilization film for the entrapment of Hb. The electrochemical property of Hb was investigated in detail. The scanning electron microscope and infrared spectroscopy were used to characterize the Hb-CS/rGO-CS nanocomposite film. Compared with our previous reports (Wang et al., 2010), the as-prepared electrode could be prepared simply, inexpensively and environmental friendly, for there were only two films on the electrode. Futhermore, we creatively introduced electrochemically reduced graphene oxide to the

fabrication of biosensor. In addition, a pair of stable and nearly symmetric redox peak was observed on the cyclic voltammetry curves of Hb. And we further studied the effect of the scanning rate and pH on the electrochemical behavior of Hb. Under the optimal conditions, the electrocatalytic performance of Hb for CH_3NO_2 was evaluated at Hb-CS/GO-CS/GCE and the CH_3NO_2 biosensor demonstrated a wide linear range, good stability and high selectivity. Therefore, a third-generation CH_3NO_2 biosensor was constructed.

2. Experimental section

2.1. Apparatus

All the electrochemical experiments were carried on a CHI660A electrochemical workstation (Shanghai Chenhua Instrument Co., Ltd.). A conventional three-electrode system, with a glassy carbon electrode (SCE) as the working electrode, a saturated calomel electrode (SCE) as the reference electrode and a platinum wire as the auxiliary electrode, was used in the electrochemical measurements. All experiments were performed under nitrogen atmosphere at room temperature, and the electrolyte was bubbled with nitrogen for 15 min to deoxygenate. A JEOL JSM7100F field emission scanning electron microscopy (SEM, Japan) was used for characterizing the prepared samples. IR spectra were measured on FT-IR 8400S spectrophotometer (Shimadu, Japan). The pH of electrolytic solutions was determined on pH s-25 acidity meter (Albert Instrument Factory, Shanghai).

2.2. Reagents and Materials

Chitosan (CS) was purchased from Aladdin reagent company, CS hydrogel was prepared by dissolving 1 mg CS in 1mL 0.1 M acetic acid (HAc), preserved in the refrigerator at 4 ℃.

Graphene oxide (GO) was provided by Sinocarbon Materials Technology Co., Ltd. (Taiyuan Shanxi), and used as received, whose concentration is 1 mg/mL. To get good cyclic voltammetry response and obtain the full realization of the electrochemical reduction process, the preparation of GO-CS composite membrane was optimized. The concentration of CS was optimized and selected as 1 mg/mL. And the optimal volume ratio of 1 mg/mL GO and 1 mg/mL CS is 1:3. Bovine hemoglobin (Hb) was obtained from Solarbio Science & Technology Co., Ltd. (Beijing, China), and the 20 mg/mL Hb stock solution was prepared by dissolving Hb in 1 mg/mL CS hydrogel. The supporting electrolyte for experiments was 0.1 M pH 7.0 phosphate buffer solution (PBS) prepared with Na_2HPO_4 and NaH_2PO_4, using NaOH and H_3PO_4 to adjust pH. Nitromethane (CH_3NO_2) was obtained from Aladdin Reagent Company, freshly prepared by directly diluted with 0.1 M pH 7.0 PBS according to the requirement. All the reagents were analytical grade and used directly without further purification. All solutions were prepared with deionized double-distilled water.

2.3. Construction of the biosensor

GCE (Ø = 3 mm) surface was polished with 0.05 μm alumina slurry, then washed with deionized water and ultrasonic cleaning successively in water, ethanol and water. To prepare the GO-CS/GCE, 5 μL resulting GO-CS dispersion was first coat onto the pretreated GCE and dry in air. Then, the GO-CS/GCE was transferred to N_2 saturated PBS (pH 7.0) solution, the GO in the GO-CS film was electrochemically reduced to rGO by performing 16 cycles continuous cyclic voltammograms from 0.2 V ~ −1.7 V at a scan rate of 50 $mV \cdot s^{-1}$, the modified electrode was expressed as rGO-CS/GCE, which would be birefly explained in the following section. After rinsing with deionized water and drying, 5 μL Hb-CS stock solution was coated on the surface of

the rGO-CS/GCE, the biosensor denoted in the text as Hb-CS/rGO-CS/GCE was fabricated. For comparison, rGO-CS/GCE, GO-CS/GCE and Hb-CS/GCE were also prepared by the same procedures.

Please, insert Fig. 1 here.

3. Results and discussions

3.1. General characterization

The surface morphologies of GO-CS and Hb-CS/rGO-CS membrane were characterized by SEM. Fig.2A shows the SEM image of the GO-CS film and it typically illustrated the morphology of thin crumpled paper, which consisted with previous reports (Wen et al., 2012; Zhou et al., 2009). From Fig.2B for the Hb-CS/rGO-CS film, we can clearly see that the near-spheroidal Hb molecules distributed uniformly on the surface of rGO-CS film, which demonstrated that Hb had been successfully immobilized on the rGO-CS film. Furthermore, it was the three-dimensional porous structure that helped maintain the natural activity of Hb and enhanced the sensitivity of the biosensor. Fig.2C (from left to right) presented the photos of as-prepared GO-CS, rGO-CS composite. The color of GO-CS is brown while that of rGO-CS is black, which was exactly used to distinguish GO-CS and rGO-CS. This is mainly because GO is brown while rGO is black (Bonanni et al., 2012). The infrared spectra of GO-CS and rGO-CS composite were shown in Fig.2D, the spectrum of GO-CS (curve a) exhibited well-defined characteristic peaks, v(O–H) = 3400 cm^{-1}, v(C=C) = 1640 cm^{-1} and v(C–O) = 1040 cm^{-1}. However, for the spectrum of rGO-CS (curve b), these characteristic peaks nearly weakened or disappeared, revealing that the typical oxygen functional groups such as hydroxyl, carbonyl and epoxy groups had been irreversibly

reduced through the electrochemical reduction. Evidently, the electrochemical reduction method in this paper was efficient and eminent. These observations have fully suggested the successful preparation of rGO-CS composite by the electrochemical reduction method (Mani et al., 2013; Unnikrishnan et al., 2013).

Please, insert Fig. 2 here.

3.2. Electrochemical reduction of GO-CS

Fig.3 showed the direct electrochemical reduction of GO-CS composite in N_2 saturated 0.1 M pH 7.0 PBS with the potential ranging from 0.2 V ~ −1.7 V (scan rate: 0.05 $V \cdot s^{-1}$). As seen in the first cycle, a broad cathodic peak at −0.3 V could be observed, in the subsequent cycles the reducing current significantly decreased to disappear, which was consistent with previous reports (Mani et al., 2013), indicating the significant reduction of oxygen functionalities of GO, such as hydroxyl, epoxy group, carboxyl group, etc (Gao et al. 2010; Ting et al., 2011). The modified electrode was denoted as rGO-CS/GCE.

The inset presented the cyclic voltammogram of the reduction of GO, a cathodic peak current appeared at −0.3 V, much lower than that of GO-CS (−0.7 V). Moreover, its peak current (150 mA) was also larger. These results may be caused by the presence of CS, which hindered the electron transfer between GO and the surface of electrode and led to a decrease in the peak current to some extent.

Please, insert Fig. 3 here.

3.3. Direct electrochemistry of Hb-CS/rGO-CS/GCE

Fig.4 showed the cyclic voltammetry of different modified electrodes in 0.1 M pH 7.0 PBS at a scan rate of 0.1 $V \cdot s^{-1}$. No redox peak was observed for GO-CS (curve c) and rGO-CS (curve d) except for a large background current. And the background current of rGO-CS/GCE was much larger than that of GO-CS/GCE, which was another powerful evidence of the successful reduction of GO to rGO. That the background current of rGO-CS modified GCE was much larger than of GO-CS modified electrode was due to the excellent conductivity of rGO, which allowed fast electron-transfer at the nanocomposite film. While GO was non-conductive, thus the GO-CS modified GCE had low background current (Unnikrishnan et al., 2013). Curve b represented the bare GCE. Whereas, a pair of stable and well defined redox peaks appeared on the CVs of Hb-CS/rGO-CS/GCE (curve e). The anodic peak potential (E_{pa}) is −0.288 V, the cathodic peak potential (E_{pc}) is −0.386 V, the formal potential ($E^{0'}$, the average of Epa and Epc) is −0.338 V *vs.* SCE, characteristic of Fe^{III}/Fe^{II} redox couple of Hb (Wang et al., 2005). Moreover, the potential difference (ΔE_p) between the anodic and cathodic peak potential was about 98 mV and the ratio of anodic peak current (I_{pa}) and cathodic peak current (I_{pc}), I_{pa}/I_{pc}, was approximately 1. These results confirmed that Hb embedded in CS/rGO-CS membrane undergone a quasi-reversible and one-electron redox electrochemical reaction (Chen et al., 2009). In comparison, the CV of Hb-CS/GCE (curve a) without rGO was extremely weak, suggesting that CS/rGO-CS could provide a conductive and suitable microenvironment for Hb, and the unique physical and chemical properties of rGO in the film effectively promoted the electron transfer between Hb and the electrode surface.

Please, insert Fig. 4 here.

3.4. Optimization of experimental conditions

3.4.1. Influence of scan rate on the electrochemical behavior of the biosensor

The cyclic voltammograms of Hb-CS/rGO-CS/GCE in deoxygenated PBS at different scan rates were also studied (Fig. S1 in the Supporting Information). With the scan rates increasing from 10 to 500 $mV \cdot s^{-1}$, the anodic and cathodic peak potentials changed slightly and peak to peak separation became larger too. Meanwhile, the cathodic and anodic peak currents were to the increasing scan rate. From the inset, it could be seen that i_{pa}-v and i_{pc}-v showed a linear relationship and the ratio of slopes (S_{ipa}/S_{ipc}) was close to 1. All these results demonstrated that the redox process of Hb immobilized in CS/rGO-CS film was surface-confined thin-layer electrochemical process. Next, the electron transfer of Hb at the Hb-CS/rGO-CS/GCE was also explored. According to the Laviron Equation (Laviron, 1979):

$$I_p = n^2F^2AvΓ^*/4RT = nFQv/4RT \qquad (1)$$

where I_p is the peak current, v is the scan rate, n is the number of electron transfer in the redox reaction (n = 1), F is Faraday constant, A is the effective surface area of modified electrode (A = 0.07 cm^{-2}), R is Molar gas constant and T is the temperature. The surface concentrations of electroactive Hb moleculars, $Γ^*$, was calculated to be 8.0×10^{-10} $mol \cdot cm^{-2}$, which was 42 times larger than the theoretical monolayer coverage (1.89×10^{-11} $mol \cdot cm^{-2}$) (Muirhead and Perutz, 1963), indicating the multilayers of Hb on the film was involved in the electron-transfer process. This value was also larger than that of GR-CS/Hb/GR/IL (7.70×10^{-10} $mol \cdot cm^{-2}$) (Wang et al., 2010), SWCNTs-Hb/GCE (9.79×10^{-11} $mol \cdot cm^{-2}$) (Ding et al., 2010) and Hb-CNDs-CS/GCE (8.78×10^{-11}

mol·cm^{-2}) (Sheng et al., 2014). The greater surface coverage was attributed to the rGO with high specific surface area and excellent high conductivity.

We further studied the relationship between redox peak potentials and scan rate, and researched the electron transfer kinetics of Hb by Laviron model (Laviron, 1979). The plots of E_{pc} and E_{pa} versus the logarithm of the scan rate was made, respectively. It was found that the peak potentials showed a slight change with scan rate changing from 10 to 50 mV·s^{-1}. At higher scan rates, however, E_{pc} and E_{pa} were linear with scan rate with slopes of 2.3RT/(1-α)nF and −2.3RT/αnF. Thus the electron transfer coefficient (α) was estimated to 0.6, and in accordance with Laviron equation (Laviron, 1979):

$$\log k_s=\alpha\log(1-\alpha)+(1-\alpha)\log\alpha-\log(RT/nFv)-\alpha(1-\alpha)nF\Delta E_p/2.3RT \quad (2)$$

The heterogeneous electron transfer rate constant (k_s) of Hb was calculated to be 6.48 s^{-1}, which was superior to that of Hb entrapped in other film, such as Fe_3O_4-CS-Hb/GCE (1.04 s^{-1}) (Zheng et al., 2009), CNC/Hb/Nafion/GCE (2.44s^{-1}) (George and Lee, 2009), Hb-Fe_3O_4-GR/GCE (0.91 s^{-1}) (He et al., 2011) and so on, suggesting that the direct electron-transfer process of Hb was fast, which would be ascribed to the excellent performance of CS/rGO-CS nanocomposite.

3.4.2. The influence of pH on the electrochemical behavior of the biosensor.

The effect of pH on the electrochemical behavior of Hb at Hb-CS/rGO-CS/GCE was explored. Fig. S2(A) displayed the CVs of Hb-CS/rGO-CS/GCE in PBS with different pH. The significant and stable redox peak could be observed. And with the pH value increasing from 5.0 to 9.0, the peak current changed significantly and reached the maximum at 7.0. Therefore pH 7.0 was chosen as the optimum pH value of electrolyte. Simultaneously, The anodic peak potential (E_{pa}) and cathodic peak potential (E_{pc}) shifted negatively, revealing that the redox process of

Hb(Fe^{III})/Hb(Fe^{II}) involved proton transfer. As shown in Fig.S2 (B), the E_{pa}, E_{pc} and formal potential ($E^{0'}$) were linearly dependent on the pH value of electrolyte with the slopes value of 35, 34, 37 mV/pH, respectively, which were lower than the theoretical value of −57.6 mV/pH (298K) in accordance with the Nernst equation for a one-proton coupled single-electron transfer reaction (Bard and Faulkner, 2001). The difference may be ascribed to the complexity of protonation process, which was greatly influenced by the protonation of amino acid residues around the heme as well as the protonation of water molecules coordinated to the central iron (Lu et al., 2007). All of the results illustrated a rapid proton transfer in the electron transfer reaction, and confirmed further that one proton (H^+) and one electron (e^-) were participate in the electrochemical reaction of Hb, noted as follow:

$$\text{Hb heme}(Fe^{III})+H^++e^- = \text{Hb heme}(Fe^{II}). \quad (3)$$

3.5. Electrochemical performance of the biosensor toward CH_3NO_2

It was well known that bioactive Hb immobilized on the electrode surface, as a heme protein, had good ability to electrocatalytically reduce O_2, TCA, NO, H_2O_2, CH_3NO_2, etc. We estimated the electrocatalytical activity of the Hb-CS/rGO-CS/GCE for the reduction of CH_3NO_2 as an example by the cyclic voltammetry. As shown in Fig.5A, a pair of characteristic redox peaks could be apparently observed on the CVs of Hb-CS/rGO-CS/GCE in PBS without CH_3NO_2 (curve a). Upon the addition of CH_3NO_2, a new reductive peak at about −0.8 V was appeared (curve d). However, there was no corresponding electrochemical response at rGO-CS/GCE in the presence of CH_3NO_2 (curve c). Obviously, the catalytic process was the electrocatalytical reduction of CH_3NO_2 by Hb, and Hb entrapped in CS/rGO-CS film kept higher catalytic activity for CH_3NO_2. In addition, the more CH_3NO_2 added, the larger the new reductive peak (data not shown). So the

Hb-CS/rGO-CS/GCE can be served as CH_3NO_2 biosensor to determine the concentration of CH_3NO_2 in the solution.

There was no doubt that the applied potential could strongly affect the current response of electrochemical biosensors. We further investigated the influence of applied potential. When potential shifted negatively from −0.4 V ~ −0.8 V, the reduction current increased significantly, indicating the sensitivity of the biosensor was greatly improved. However, too negative working potential was also accompanied with increasing interference. As a result, −0.8 V was chosen as the optimum applied potential for amperometric detection of CH_3NO_2. Fig.5B presented the amperometric response of Hb-CS/rGO-CS/GCE to CH_3NO_2 with successive addition of a certain concentration of CH_3NO_2 (once every 40 s) to a continuous stirring and deoxygenated PBS. Once CH_3NO_2 added, the reduction current increased quickly and reached a steady state within about 3s. So fast response was due to the good conductivity of rGO and the easy diffusion of substrate in Hb-CS/rGO-CS membrane. The calibration curves of current against the CH_3NO_2 concentration was shown in the inset of Fig 5 B, showing an excellent linear relationship from 5 μM to 1.46 mM with a correlation coefficient of 0.999, and the detection limit was 1.5 μM (S/N = 3). The linear concentration range spanned three orders of magnitude from micromolar to millimolar, which was much wider than that of 4.47×10^{-8}～4.45×10^{-6} M at Hb-CMC/IL/MWNTs (Wang et al., 2012) and 2.0×10^{-9}～2.3×10^{-7} M at GR-CS/Hb/GR/IL/GCE(Wang et al., 2010). Such wider linear range further clarified that the Hb-CS/rGO-CS nanocomposite with a three-dimensional structure effectively kept the active of Hb and enhanced the catalytic performance of Hb for CH_3NO_2. It is clearly that the Hb-CS/rGO-CS/GCE had wide range of measurement and high sensitivity, and can be widely used in practice.

It could be found that the response current gradually tended to level off when CH_3NO_2 was continuously added to a certain degree, displaying the typical characteristics of Michaelis-Menten kinetic mechanism. According to the Lineweaver-Burk equation (Kamin and Wilson, 1980), the apparent Michaelis-Menten constant (K_m^{app}) of the biosensor was calculated to be about 3.57 mA. It was worth noting that the low value of K_m^{app} revealed Hb in CS/rGO-CS film remained its good biocatalytic activity and had extremely high affinity to CH_3NO_2.

Please, insert Fig. 5 here.

3.6. The selectivity, reproducibility and stability of the CH_3NO_2 biosensor

Selectivity is an important indicator for the practical application of biosensors. The effect of interfering substances on the 4.5×10^{-5} M CH_3NO_2 measurement was evaluated by the current-time curve. As shown in Fig. 6, the 100-fold concentration of NO_3^-、HPO_4^{2-}、C_6H_{14}、NO_2^- produced no amperometric response and did not interfere the CH_3NO_2 test. The high selectivity of the resulting biosensor can be ascribe to the proper working potential and the inherent selection of Hb.

The reproducibility of the biosensor was also researched by detecting 0.1 mM CH_3NO_2 in pH 7.0 PBS. The relative standard deviation (RSD) was 3.7% for 10 consecutive determinations using the same Hb-CS/rGO-CS/GCE. Five electrodes, prepared by the same method, showed similar current response to 0.1 mM CH_3NO_2 with a RSD of 5.8%, which suggested the satisfying reproducibility of the biosensor for CH_3NO_2 measurement. The stability was firstly examined by evaluating the CV peak currents of Hb, after scanning for 100 cycles, the well-defined redox peaks kept unchanged and only the peak current decreased slightly. The Hb-CS/rGO-CS/GCE could retain 90% of initial current response after stored for 10 days in the refrigerator at 4℃. The good

reproducibility and stability demonstrated that immobilization of Hb in CS/rGO-CS nanocomposite was an efficient and effective fabrication process.

Please, insert Fig. 6 here.

3.7. Practical applications of CH_3NO_2 biosensor

To evaluate the potential applications of the biosensor, the Hb-CS/rGO-CS/GCE was directly used to detect of CH_3NO_2 in freshwater samples. The CH_3NO_2 content in the collected samples was too low to be measured by the biosensor. So the standard addition method was performed. We determined the current response of the real samples by adding different concentration of standard CH_3NO_2 solution to 9 mL tested water served as electrolyte. The results were recorded in Table 1 in the Supporting information, the recoveries were 95.4～102.8%, indicating that the reliability and broad prospects of the CH_3NO_2 biosensor in practical applications.

4. Conclusions

In this paper, electrochemically reduced graphene oxide associated with biopolymer (CS) was firstly used to immobilize Hb and to fabricate a novel CH_3NO_2 biosensor. The unique Hb-CS/GO-CS membrane was extremely stable, the employment of rGO and CS with high conductivity and biocompatibility could retain the biological activity of Hb and greatly promote the direct electron transfer of Hb. Therefore, the biosensor showed a good performance for CH_3NO_2 determination with a wide linear range of 5 μM ~ 1.46 mM and a low detection limit of 1.5 μM. Meanwhile, the biosensor had acceptable stability, reproducibility and selectivity, which could be prepared simply and inexpensively, providing the possibility for the analysis of the CH_3NO_2 in complex real samples. What's more, the entrapment combined rGO and CS is

expected to construct more bioelectrochemical devices.

Notes

The authors declare no competing financial interest.

Acknowledgments

This work was financially supported by the National Natural Science Foundation of China (Grant No. 21475032, 21175032, 21405035), the Natural Science Fund for Creative Research Groups of Hubei Province of China (No. 2014CFA015).

References

Allen, M.J., Tung, V.C., Kaner, R.B., 2010. Chem. Rev. 110(1), 132-145.

Alwarappan, S., Erdem, A., Liu, C., Li, C.Z., 2009. J. Phys. Chem. C 113(20), 8853-8857.

Alwis, K.U., Blount, B.C., Silva, L.K., Smith M.M., Loose, K.H., 2008. Environ. Sci. Technol. 42 (7), 2522–2527.

Bard, A.J., Faulkner, L.R., 2001. Electrochemical Methods: Fundamentals and Applications. John Wiley and Sons, NewYork. pp. 591.

Bonanni, A., Chua, C.K., Zhao, G.J., Sofer, Z., Pumera, M., 2012. Acs Nano 6(10), 8546-8551.

Chen, X., Fu, C.L., Yang, W.S., 2009. Analyst. 134(10), 2135-2140.

Ding, Y., Wang, Y., Lei, Y., 2010. Biosens. Bioelectron. 26(2), 390-397.

Dong, H.F., Zhu, Z., Ju, H.X., Yan, F., 2012. Biosens. Bioelectron. 33(1), 228-232.

Gao, X.F., Jang, J., Nagase, S., 2010. J. Phys. Chem. C 114(2), 832-842.

Geim, A.K., Novoselov, K.S., 2007. Nat. Mater. 6(3), 183-191.

George, S., Lee, H.K., 2009. J. Phys. Chem.B 113(47), 15445-15454.

Guo, H.L., Wang, X.F., Qian, Q.Y., Wang, F.B., Xia, X.H., 2009. Acs Nano 3(9), 2653-2659.

He, Y.P., Sheng, Q.L., Zheng, J.B., Wang, M.Z., Liu, B., 2011. Electrochim. Acta. 56(5), 2471-2476.

Jones, L.R., Riddick, J.A., 1951. Anal. Chem. 23(2), 349-351.

Kamin, R.A., Wilson, G.S., 1980. Anal. Chem. 52(8), 1198-1205.

Kang, X.H., Wang, J., Wu, H., Aksay, I.A., Liu, J., Lin, Y.H., 2009. Biosens. Bioelectron. 25(4), 901-905.

Laviron, E., 1979. J. Electroanal. Chem. 101(1), 19-28.

Léger, C., Bertrand, P., 2008. Chem. Rev. 108(7), 2379-2438.

Li, D., Muller, M.B., Gilje, S., Kaner, R.B., Wallace, G.G., 2008. Nat. Nanotechnol. 3(2), 101-105.

Lin, D., Wu, J., Wang, M., Yan, F., Ju H.X., 2012. Anal. Chem. 84, 3662–3668.

Liu, H.H., Tian, Z.Q., Lu, Z.X., Zhang, Z.L., Zhang, M., Pang, D.W., 2004. Biosens. Bioelectron. 20(2), 294-304.

Lu, Q., Hu, C.G., Cui, R., Hu, S.S., 2007. J. Phys. Chem. B 111(33), 9808-9813.

Lu, X.B., Hu, J.Q., Yao, X., Wang, Z.P., Li, J.H., 2006. Biomacromolecules. 7(3), 975-980.

Mani, V., Devadas, B., Chen, S.M., 2013. Biosens. Bioelectron. 41, 309-315.

Meaney, M.S., McGuffin, V.L., 2008. Anal. Chim. Acta. 610(1), 57-67.

Muirhead, H., Perutz, M.F., 1963. Nature 199(489), 633-639.

Novoselov, K.S., Geim, A.K., Morozov, S.V., Jiang, D., Zhang, Y., Dubonos, S.V., Grigorieva, I.V., Firsov, A.A., 2004. Science 306(5696), 666-669.

Page, E.H., Pajeau, A.K., Arnold, T.C., Fincher, A.R., Goddard, M.J., 2001. Am. J. Ind. Med. 40(1), 107-113.

Park, S., Ruoff, R.S., 2009. Nat. Nanotechnol. 4(4), 217-224.

Peniche, C., Arguelles-Monal, W., Peniche, H., Acosta, N., 2003. Macromol. Biosci. 3(10), 511-520.

Sabourin, J.L., Dabbs, D.M., Yetter, R.A., Dryer, F.L., Aksay, I.A., 2009. Acs Nano 3(12), 3945-3954.

Shan, C.S., Yang, H.F., Song, J.F., Han, D.X., Ivaska, A., Niu, L., 2009. Anal. Chem. 81(6), 2378-2382.

Sheng, M.L., Gao, Y., Sun, J.Y., Gao, F., 2014. Biosens. Bioelectron. 58, 351-358.

Stankovich, S., Dikin, D.A., Dommett, G.H.B., Kohlhaas, K.M., Zimney, E.J., Stach, E.A., Piner, R.D., Nguyen, S.T., Ruoff, R.S., 2006. Nature 442(7100), 282-286.

Sun, W., Hou, F., Gong, S.X., Han, L, Wang, W.C., Shi, F., Xi, J.W., Wang, X.L., Li, G.J., 2015. Sens. Actuators B. 219, 331–337.

Ting, S.W., Periasamy, A.P., Chen, S.M., Saraswathi, R., 2011. Int. J. Electrochem. Sc. 6(10), 4438-4453.

Unnikrishnan, B., Palanisamy, S., Chen, S.M., 2013. Biosens. Bioelectron. 39(1), 70-75.

Wang, L., Zhang, X.H., Xiong, H.Y., Wang, S.F., 2010. Biosens. Bioelectron. 26(3), 991-995.

Wang, S.F., Chen, T., Zhang, Z.L., Shen, X.C., Lu, Z.X., Pang, D.W., Wong, K.Y., 2005. Langmuir. 21(20), 9260-9266.

Wang, Y.M., Xiong, H.Y., Zhang, X.H., Ye, Y., Wang, S.F., 2012. J. Electroanal. Chem. 674, 17-22.

Wen, W., Chen, W., Ren, Q.Q., Hu, X.Y., Xiong, H.Y., Zhang, X.H., Wang, S.F., Zhao, Y.D., 2012. Sens. Actuators B 166, 444-450.

Xu, H., Xiong, H.Y., Zeng, Q.X., Jia, L., Wang, Y., Wang, S.F., 2009. Electrochem. Commun. 11(2), 286-289.

Zhang, M.G., Smith, A., Gorski, W., 2004. Anal. Chem. 76(17), 5045-5050.

Zheng, N., Zhou, X., Yang, W.Y., Li, X.J., Yuan, Z.B., 2009. Talanta 79(3), 780-786.

Zhou, M., Zhai, Y.M., Dong, S.J., 2009. Anal. Chem. 81(14), 5603-5613.

Highlights

1. Graphene was produced by the electrochemical reduction method, which is green and efficient.

2. A biosensor based on electrochemically-reduced graphene oxide, CS and Hb was constructed.

3. The biosensor demonstrated a wide linear range of and a low detection limit for CH_3NO_2 detection.

4. The biosensor has been applied in real samples, with high selectivity and stability.

Figures

Fig. 1. Schematic illustration of the assembly process of Hb-CS/rGO-CS/GCE.

Fig. 2. SEM images of (A) GO/CS, (B) Hb-CS/rGO-CS on the glassy carbon. (C) colloidal suspension of GO-CS and rGO-CS (from left to right). (D) The infrared spectra of (a) GO-CS, (b) rGO-CS.

Fig. 3. Cyclic voltammogram of electrochemical reduction of GO-CS/GCE to rGO-CS/GCE in N_2 saturated PBS (pH 7.0), Scan rate: 0.05 $V \cdot s^{-1}$. Inset: Electrochemical reduction of GO/GCE under identical experimental conditions.

Fig. 4. Cyclic voltammograms of (a)Hb-CS/GCE, (b)bare GCE, (c)GO-CS/GCE, (d)rGO-CS/GCE, (e)Hb-CS/rGO-CS/GCE in pH 7.0 PBS at a scan rate of 0.1 $V \cdot s^{-1}$.

Fig. 5. (A) CVs at 0.1 $V \cdot s^{-1}$ in 0.1 M deoxygenated pH 7.0 PBS for (a) rGO-CS/GCE, (c) Hb-CS/rGO-CS/GCE without CH_3NO_2， (b)rGO-CS/GCE, (d)Hb-CS/rGO-CS/GCE in buffer containing 9mM CH_3NO_2. (B) Amperometric response of Hb-CS/rGO-CS/GCE to upon successive additions of CH_3NO_2 into stirring 0.1 M pH 7.0 PBS. Applied potential: −0.70 V. Inset: the corrected curves of catalytic current against CH_3NO_2 concentration for Hb-CS/rGO-CS/GCE in 0.1 M pH 7.0 PBS. Error bars were obtained from three experiments and the RSD was less than 3.5%.

Fig. 6. Amperometric response of Hb-CS/rGO-CS/GCE to CH_3NO_2 in the presence of some co-existing compounds in PBS (pH 7.0), applied potential: -0.80 V.

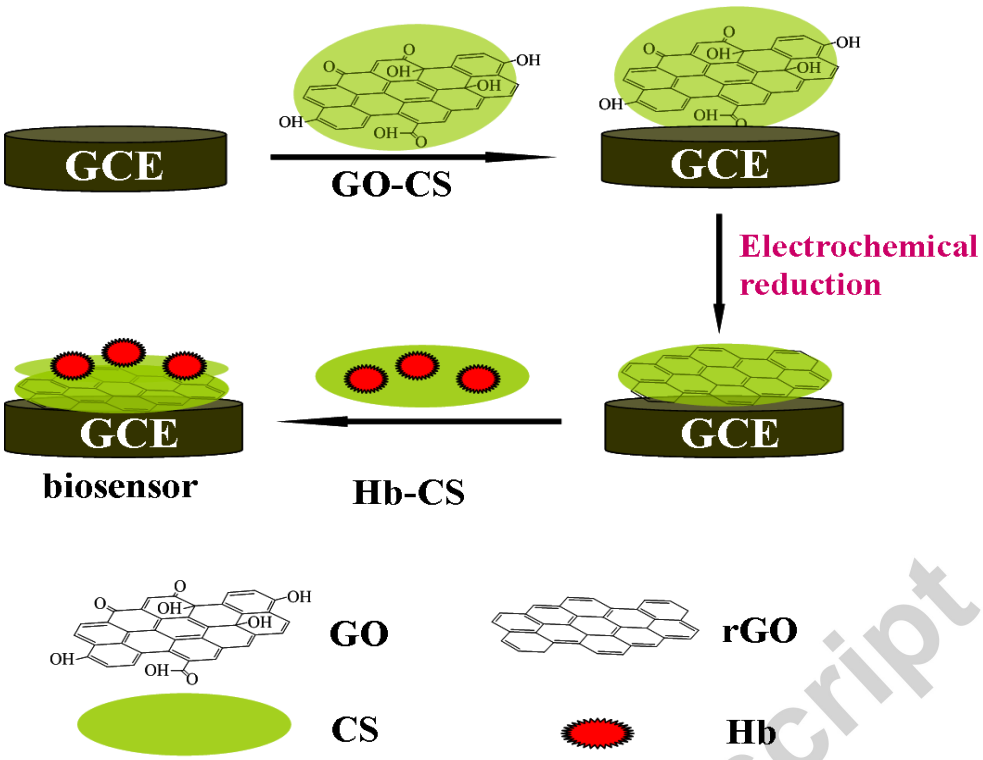

Fig. 1.

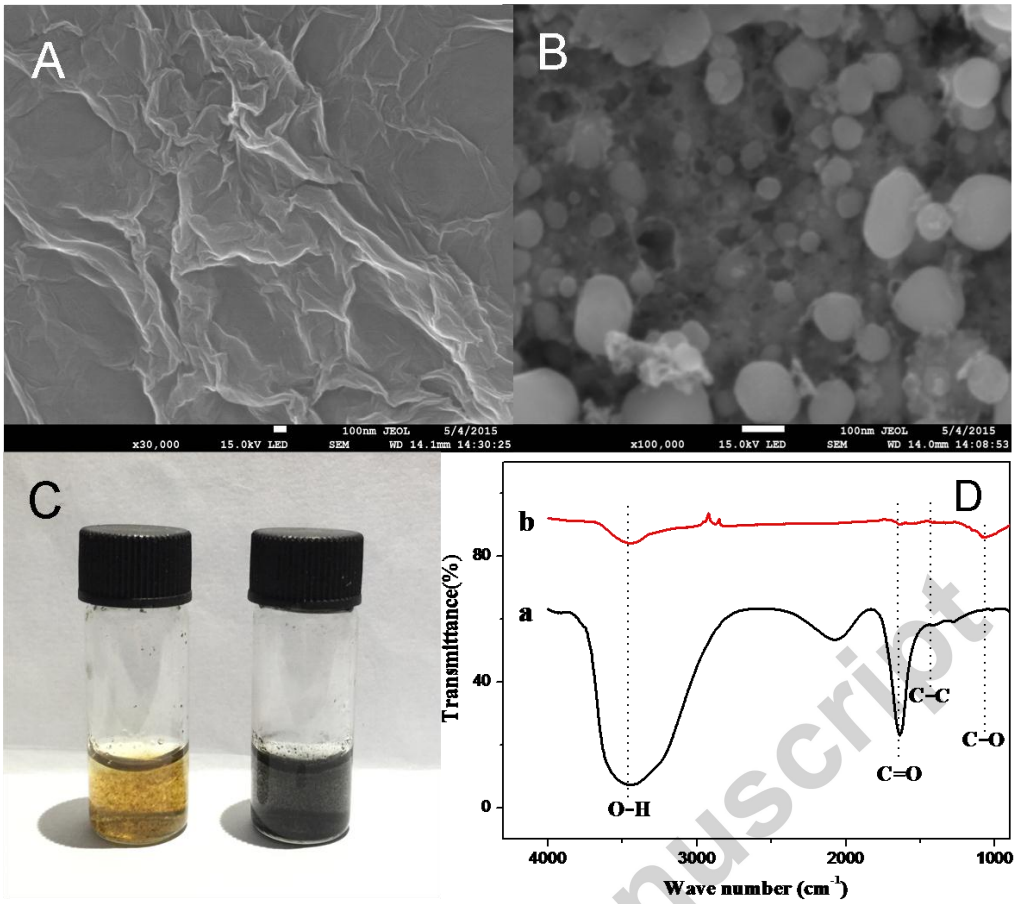

Fig. 2.

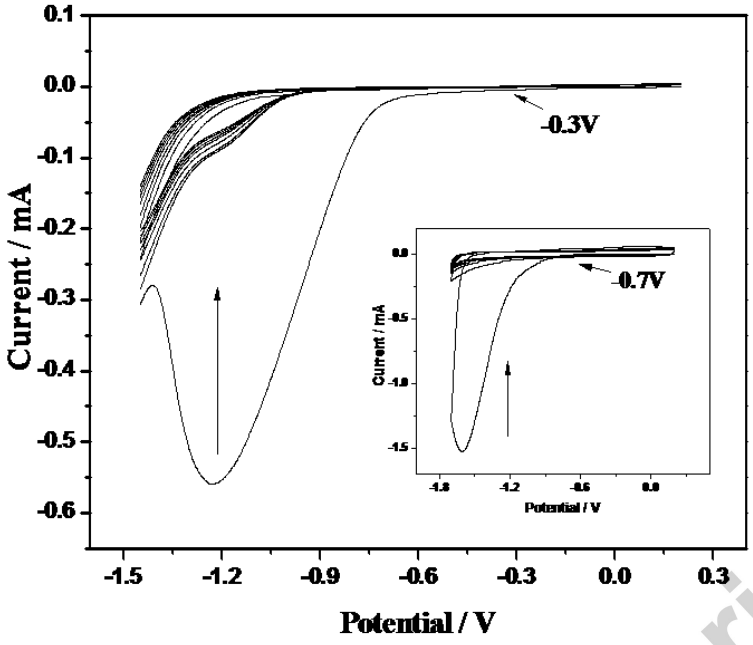

Fig. 3.

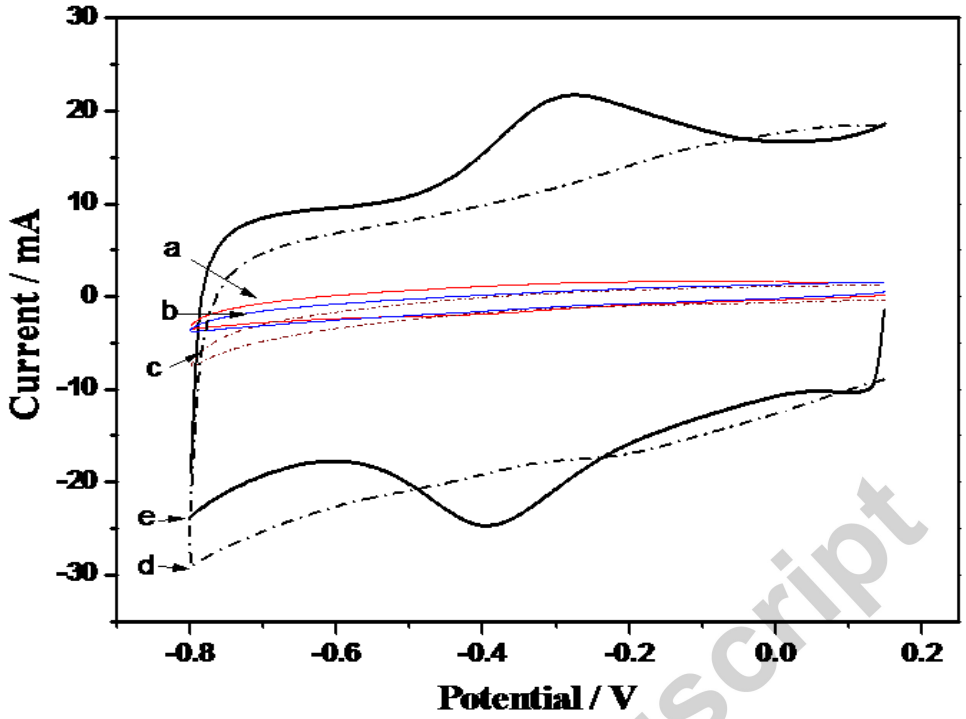

Fig. 4.

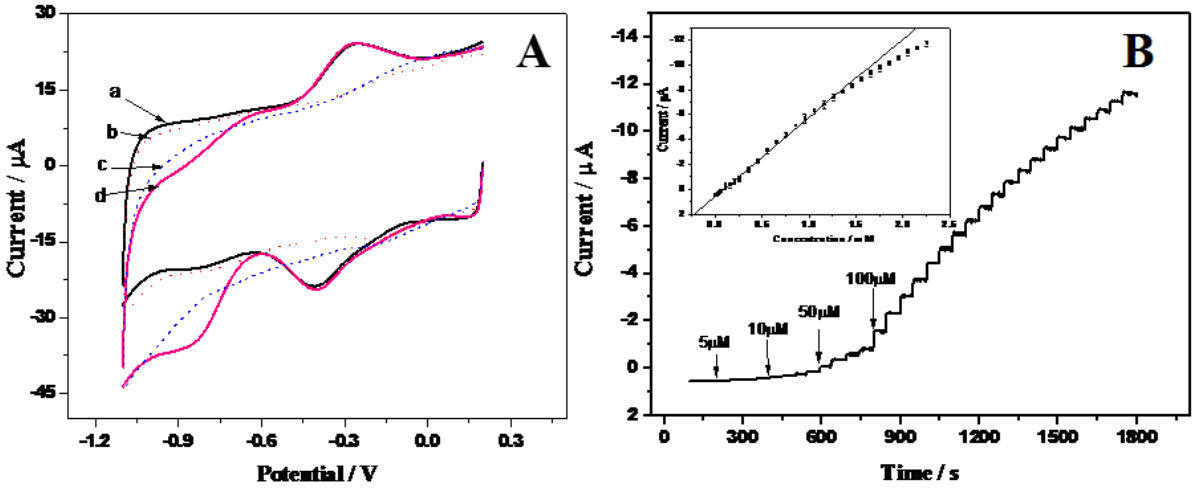

Fig. 5.

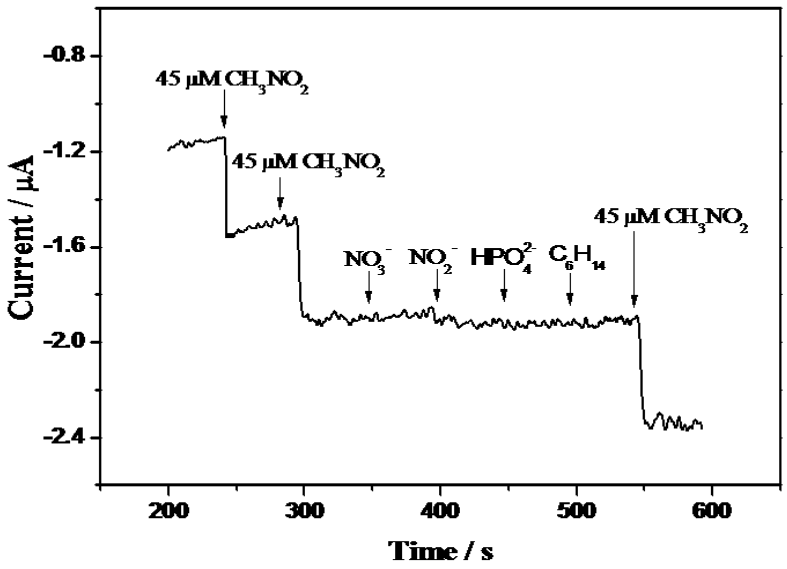

Fig. 6.